University of Groningen

Disorder and interchain interactions in Peierls systems

Figge, Marc Thilo Günter

2 Models for Peierls Systems

We introduce a continuum model for weakly disordered Peierls chains which represents the starting point of our studies in Chapter 3 and Chapter 5. Several properties of this model are discussed in two limiting cases: First, in the absence of electron-electron interactions and disorder our model reduces to the Takayama−Lin-Liu−Maki (TLM) model for an isolated Peierls chain. The TLM model allows one to study analytically the effect of the Peierls distortion and the nature of topological excitations. Second, we discuss the Fluctuating Gap Model (FGM) for an isolated Peierls chain which is an often used model to account for disorder. We illustrate how the Peierls gap turns into a pseudogap due to the presence of disorder and discuss the underlying phenomenology of the FGM concerning the role of interchain interactions. Finally, we discuss the effect of electron correlations and interchain interactions on the dimerization of the lattice in Peierls chains.

A first reading of this chapter should include Section 2.1 and Section 2.4, while the other sections may be skipped by the reader who is familiar with the basic properties of the TLM model and the FGM.

*The continuum model for a disordered Peierls chain has been discussed in Physical Review B **57**, 2861 (1998).*

2.1 Continuum model of disordered Peierls chains

In this section we derive a continuum model to describe weakly disordered Peierls systems with a doubly degenerate ground state. As an example of a Peierls system, we considered in Chapter 1 the conjugated polymer *trans*-polyacetylene. A *trans*-polyacetylene chain consists of carbon-hydrogen units (see Figure 1-1 (c)). Three of the four electrons in the outer shell of each carbon atom form bonds with the hydrogen atom and the two neighboring carbon atoms. This so-called sp^2-hybridization results in a planar zigzag arrangement of the carbon atoms along the chain direction. The remaining fourth electron of each carbon atom can propagate along the polymer chain and is called π-electron, as it occupies the $2p_z$-orbital perpendicular to the chain plane.

We start with the derivation of the continuum model by considering a tight binding model which describes the hopping of electrons along a chain of atoms. The electron hopping amplitudes depend on the interatomic distances and the relative orientation of the electronic orbitals on neighboring atoms. Therefore, the hopping amplitudes are affected by both the lattice motion (the displacement of the atoms parallel to the chain) and conformational disorder arising from chain twists. In Figure 2-1 we give a simplified picture of a *trans*-polyacetylene chain with conformational disorder. The right part of the chain is twisted over an angle ϕ with respect to its left part.

Let t_0 denote the hopping amplitude between neighboring atoms in a perfect rigid chain of equidistant atoms with lattice constant a. Then, in the presence of atomic displacements and
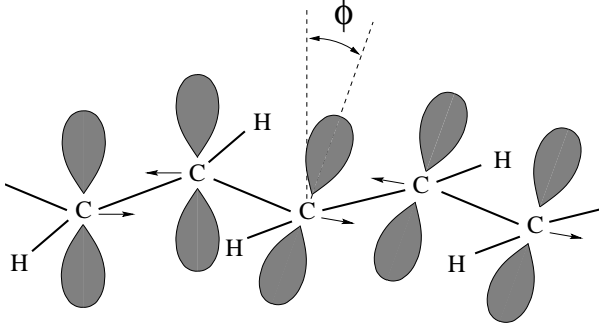
Figure 2-1: *Conformational disorder in a trans-polyactylene chain. The arrows indicate the displacements u_n from equidistant atom positions describing a bond-length alternation. A random chain twist with angle ϕ changes the relative orientation between neighboring π-orbitals. The electron hopping amplitude on the twisted bond is reduced by a factor $\cos \phi$.*

conformational disorder, the hopping amplitude between site n and $n+1$ reads

$$t_{n,n+1} = t_0 + \alpha(u_n - u_{n+1}) + \delta t_{n,n+1} . \tag{2.1}$$

Here, the second term is the electron-lattice interaction, which is of the same type as in the Su—Schrieffer—Heeger (SSH) model [1]. The coupling constant is given by α and u_n is the displacement of the n'th atom from its uniform-lattice position. The third term in Eq. (2.1) is a random contribution resulting from the conformational disorder. While the lattice displacements u_n are dynamic variables, we will assume that the fluctuations $\delta t_{n,n+1}$ are frozen ("quenched" disorder) and small compared to the hopping amplitude of the undistorted lattice, $\delta t_{n,n+1} \ll t_0$ (weak disorder).

The kinetic energy of the electrons for a chain of length L with $N = L/a$ sites is described by the tight-binding Hamiltonian

$$\begin{aligned} H_{el} &= -\sum_{m,\sigma} \left[\bar{t}(2ma) + \frac{1}{2}\Delta(2ma) \right] (c^\dagger_{2m,\sigma} c_{2m-1,\sigma} + h.c.) + \\ &\quad -\sum_{m,\sigma} \left[\bar{t}(2ma) - \frac{1}{2}\Delta(2ma) \right] (c^\dagger_{2m,\sigma} c_{2m+1,\sigma} + h.c.) , \end{aligned} \tag{2.2}$$

where $c_{n,\sigma}$ $(c^\dagger_{n,\sigma})$ is the fermionic operator which annihilates (creates) an electron with spin projection σ at site n. We distinguish between even, $n = 2m$, and odd, $n = 2m+1$, sites where $m = 1, 2, ..., M$ and $M = N/2$. Furthermore, we defined

$$\begin{aligned} \bar{t}(2ma) &= \frac{1}{2}\left(t_{2m-1,2m} + t_{2m,2m+1}\right) \tag{2.3} \\ &= t_0 + \frac{\alpha}{2}(u_{2m-1} - u_{2m+1}) + \frac{1}{2}\left(\delta t_{2m-1,2m} + \delta t_{2m,2m+1}\right) , \end{aligned}$$

and

$$\Delta(2ma) = t_{2m-1,2m} - t_{2m,2m+1} \equiv \Delta_{lat}(2ma) + \eta(2ma) . \tag{2.4}$$

The alternating part of the hopping amplitudes, $\Delta(2ma)$, represents the Peierls order parameter. It consists of two contributions, where the first one is the lattice dimerization,

$$\Delta_{lat}(2ma) = \alpha\,(u_{2m-1} - 2u_{2m} + u_{2m+1})\,, \tag{2.5}$$

which describes the alternating part of the hopping amplitude determined by the shifts u_n of the atoms. This is the usual order parameter of the SSH model [1]. The second part of the Peierls order parameter Eq. (2.4) reflects the disorder,

$$\eta(2ma) = \delta t_{2m-1,2m} - \delta t_{2m,2m+1}\,. \tag{2.6}$$

Note, that while the random chain twists always decrease the hopping amplitudes ($\delta t_{n,n+1} < 0$), $\eta(2ma)$ can be both positive and negative, as it is the alternating part of the fluctuations.

The energy of the lattice is independent of the electronic disorder and depends only on the atomic displacements u_n. We treat the lattice classically, i.e., we disregard the lattice kinetic energy, which is reasonable for chains of sufficiently heavy atoms. (It should be noted that for *trans*-polyacetylene, which consists of relatively light CH-groups, quantum lattice effects may be rather important [2]). Taking only the elastic coupling between nearest neighbors into account, we write the potential lattice energy within the harmonic approximation,

$$E_{lat} = \frac{K}{2} \sum_m \left[(u_{2m-1} - u_{2m})^2 + (u_{2m} - u_{2m+1})^2 \right]\,, \tag{2.7}$$

where K is the nearest-neighbor spring constant.

To derive the continuum version of the electron Hamiltonian Eq. (2.2), we consider electrons close to the Fermi surface in the case of zero disorder ($\delta t_{n,n+1} = 0$). It is straightforward to obtain the electron energy spectrum, which we will denote by H_{el}^0 in this limit. The operator $c_{n,\sigma}$ and the atomic displacement u_n at site n have the Fourier representations,

$$c_{n,\sigma} = \sqrt{\frac{a}{L}} \sum_k e^{ikan} c_{k,\sigma} \tag{2.8}$$

with electron momentum $|k| \le \pi/a$, and

$$u_n = \sqrt{\frac{a}{L}} \sum_q e^{iqan} Q_q \tag{2.9}$$

with phonon momentum $|q| \le \pi/a$. We readily obtain H_{el}^0 in the form:

$$H_{el}^0 = \sum_{k,\sigma} \varepsilon(k)\, c_{k,\sigma}^\dagger c_{k,\sigma} + \sum_{k,q,\sigma} g(k,q)\, Q_q\, c_{k,\sigma}^\dagger c_{k-q,\sigma}\,. \tag{2.10}$$

Here, we introduced the electron energy spectrum in the absence of electron-lattice interaction ($\alpha = 0$),

$$\varepsilon(k) = -2\,t_0 \cos(ka)\,, \tag{2.11}$$

and the electron-lattice coupling

$$g(k,q) = 4\,i\,\alpha\,\sqrt{\frac{a}{L}} \cos\left(k - \frac{q}{2}\right) \sin\left(\frac{q}{2}\right)\,. \tag{2.12}$$
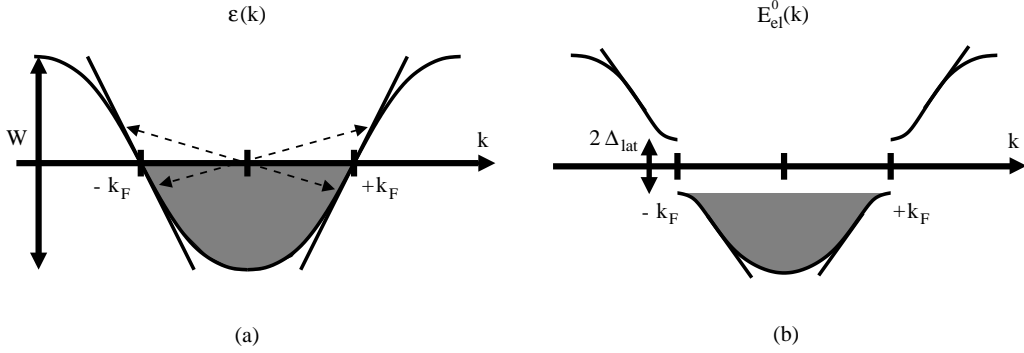
Figure 2-2: *(a) Electronic energy spectrum $\varepsilon(k)$ of a one-dimensional chain in the absence of disorder and electron-lattice interactions (solid curve). Close to the Fermi points $\pm k_F$ the electron dispersion can be linearized (solid lines). Electron-lattice interactions result in backward-scattering with $q = 2k_F$, as indicated by the dashed arrows. (b) Due to the backward-scattering the electronic energy spectrum $E_{el}^0(k)$ contains a gap $2\Delta_{lat}$ at the Fermi points. Opening the gap lowers the system's electronic energy and turns a metal into a Peierls semiconductor.*

The electron band $\varepsilon(k)$ has a width $W = 4t_0$ and is plotted in Figure 2-2 (a). For half-filling, the Fermi points are located at $\pm k_F = \pm\pi/(2a)$ and the chain is conducting. Close to the Fermi points the energy dispersion of the electrons can be linearized,

$$\varepsilon(\kappa) \approx \pm v_F \sin(k_F a)\,\kappa \, , \tag{2.13}$$

with the Fermi velocity $v_F = 2at_0$ and the electron momentum κ measured from k_F.

In the vicinity of the Fermi points, the interaction between the electrons and the lattice, $g(k, q)$, describes forward- and backward-scattering processes. Forward-scattering involves electron states which are close to the same Fermi point, in which case the coupling reads

$$g_{fw}(\kappa, q \ll k_F) \approx 4i\,\alpha \sqrt{\frac{a}{L}} \left(\frac{q^2}{4} - \frac{\kappa q}{2} \right) \, . \tag{2.14}$$

The main effect of forward-scattering is a renormalization of the electron velocity v_F, while the electron energy spectrum remains qualitatively unchanged. The effect of backward-scattering, however, is more dramatic, as it gives rise to the Peierls instability introduced in Chapter 1. Backward-scattering couples occupied electron states close to the Fermi point $+k_F$ $(-k_F)$ to the unoccupied states close to $-k_F$ $(+k_F)$ by

$$g_{bw}(\kappa, q \approx 2k_F) \approx 4i\,\alpha \sqrt{\frac{a}{L}} \sin(k_F a) \left(1 + \frac{\kappa(q - 2k_F)}{2} \right) \, . \tag{2.15}$$

In the case of a half-filled system, the Peierls distortion has wave vector $2k_F = \pi/a$, which corresponds to a bond-length alternation,

$$u_n = -(-1)^n\,u \, , \tag{2.16}$$

where we defined $u \equiv -Q_{2k_F} \sqrt{a/L}$. The spatial period of the distorted lattice is $2a$, exactly twice the original one, and the half-filled chain is referred to as a commensurability 2 system. Since it is the bond charge that is alternating in a commensurability 2 system, the charge density wave (CDW) is more precisely called a bond order wave (BOW). We briefly note, that Eq. (2.16) implies $u_{N+1} = (-1)^N u_1$ for a chain with N sites. Thus, if we impose periodic boundary conditions $u_{N+1} = u_1$, a misfit at the chain ends in chains with an odd number of sites is prevented only, if u changes sign somewhere along the chain. We discuss the topological meaning of the boundary conditions in Section 2.2.2, while here we consider for simplicity a chain with periodic boundary conditions and an even number of sites N.

It follows from Eq. (2.16) that the alternating part of the hopping amplitude Eq. (2.5) is given by a constant value, $\Delta_{lat}(2ma) = \Delta_{lat}$ with

$$\Delta_{lat} = 4\alpha u . \tag{2.17}$$

Taking only the backward-scattering with $q = 2k_F$ into account, the Hamiltonian Eq. (2.10) now reduces to

$$H_{el}^0 \approx \sum_{k_F, \kappa, \sigma}{}' \sin(k_F a) \left[v_F \kappa\, c_{k_F+\kappa,\sigma}^\dagger c_{k_F+\kappa,\sigma} - i\, \Delta_{lat}\, c_{k_F+\kappa,\sigma}^\dagger c_{-k_F+\kappa,\sigma} \right] \tag{2.18}$$

in the vicinity of the Fermi points $k_F = \pm\pi/(2a)$. The prime on the summation in Eq. (2.18) indicates that, due to the linearized electron dispersion Eq. (2.13), it is restricted to $|\kappa| \leq \Lambda$. The momentum cut-off $\Lambda \sim W/(2v_F)$ ensures that the density of electron states is conserved when the electron dispersion Eq. (2.11) is linearized and replaced by Eq. (2.13).

From a diagonalization of Eq. (2.18), we obtain the electron energy spectrum

$$E_{el}^0(\kappa) = \pm\sqrt{(v_F\kappa)^2 + \Delta_{lat}^2} , \tag{2.19}$$

which has a gap of size $2\Delta_{lat}$ at $\pm k_F$. The energy gap between occupied and unoccupied states lowers the energies of the occupied levels and, thus, decreases the total electron energy. We plot $E_{el}^0(\kappa)$ in Figure 2-2 (b), which shows that the chain is insulating at zero temperature. Of course, the Peierls instability only takes place, if the gain in the electron energy due to the lattice distortion exceeds the loss in the lattice energy Eq. (2.7) which, for the bond length alternation Eq. (2.16), is given by

$$E_{lat} = \frac{K}{2} \sum_{m=1}^{M} \frac{\Delta_{lat}^2}{2\alpha^2} . \tag{2.20}$$

That this is the case, was first shown by Peierls [3]. In Section 2.2.1 we will consider this question in more detail within the Takayama–Lin-Liu–Maki (TLM) model.

In the spirit of the above considerations, we derive the continuum model for Peierls systems including both electron-lattice interaction and electronic disorder. The reduction of the Hamiltonian Eq. (2.2) to the continuum model uses the fact that the electron energy dispersion is linear close to the Fermi points $\pm k_F$. This implies the condition of weak coupling (or small α), such that the relevant electron states are close to Fermi points with $\kappa a \sim 2\Delta_{lat}/W \ll 1$ for which the linearization of Eq. (2.11) does hold (see Figure 2-2). The electron operator

$c_{n,\sigma}$, as given by Eq. (2.8), is then represented by a product of two factors around each Fermi point, namely, one factor which varies fast along the chain on the scale of the lattice constant $a \sim k_F^{-1}$, while the second factor is a slowly varying function related to the small deviation κ of the electron momentum from k_F. The transformation from the discrete to the continuum model for the operator Eq. (2.8) is given by

$$c_{2m,\sigma} = \sqrt{a}\Big(e^{i2mak_F}\psi_{R,\sigma}(x_{2m}) - ie^{-i2mak_F}\psi_{L,\sigma}(x_{2m})\Big),$$

$$\tag{2.21}$$

$$c_{2m\pm1,\sigma} = \sqrt{a}\Big(1 \pm a\frac{d}{dx_{2m}}\Big)\Big(e^{i(2m\pm1)ak_F}\psi_{R,\sigma}(x_{2m}) - ie^{-i(2m\pm1)ak_F}\psi_{L,\sigma}(x_{2m})\Big).$$

Here, the fermionic operators $\psi_{R\sigma}(x_{2m})$ and $\psi_{L\sigma}(x_{2m})$ are the slowly varying functions that are defined at each second bond, $x_{2m} = 2ma$, and correspond to electrons moving, respectively, to the right and to the left. In what follows we will use the spinor notation

$$\Psi_{\sigma}(x) \equiv \begin{pmatrix} \psi_{R,\sigma}(x) \\ \psi_{L,\sigma}(x) \end{pmatrix} \tag{2.22}$$

to describe right- and left-moving electrons simultaneously.

Applying the transformation Eq. (2.21) and changing $\sum_m$ into $\int \frac{dx}{2a}$, we obtain the desired continuum analog of the electron Hamiltonian Eq. (2.2) in the compact form

$$H_{el}[\Delta_{lat}(x),\eta(x)] = \sum_{\sigma} \int dx\, \Psi_{\sigma}^{\dagger}(x)\, \hat{h}(x)\, \Psi_{\sigma}(x)\ , \tag{2.23}$$

with the Dirac-type Hamiltonian

$$\hat{h}(x) = \frac{v_F}{i}\frac{d}{dx}\sigma_3 + \Delta(x)\sigma_1\ . \tag{2.24}$$

Here, σ_1 and σ_3 are the Pauli matrices. The first term in Eq. (2.24) describes the free propagation of right- and left-moving electrons with the Fermi velocity $v_F = 2at_0$, where we neglected the weak spatial dependence of the hopping amplitude Eq. (2.3). The second term in Eq. (2.24) contains the order parameter Eq. (2.4) and describes the backward-scattering of right- (left-) into left- (right-) moving electrons due to both the lattice distortion and the disorder:

$$\Delta(x) = \Delta_{lat}(x) + \eta(x)\ . \tag{2.25}$$

Here, the lattice distortion

$$\Delta_{lat}(x) = 4\alpha u(x) \tag{2.26}$$

contains only the slowly varying part $u(x)$ of the atomic displacements Eq. (2.16). Throughout this thesis, we will assume $\eta(x)$ to be white noise disorder of strength A,

$$\langle \eta(x)\eta(y)\rangle = A\,\delta(x-y)\ . \tag{2.27}$$

Next, it follows from Eq. (2.20) that the harmonic lattice energy in the continuum limit is given by

$$E_{lat}[\Delta_{lat}(x)] = \frac{1}{\pi\lambda v_F}\int dx\, \Delta_{lat}(x)^2\ , \tag{2.28}$$

where we introduced the dimensionless electron-lattice coupling constant

$$\lambda \;=\; \frac{4\,\alpha^2}{\pi\,t_0\,K}\;.\tag{2.29}$$

In conclusion, the Hamiltonian of the continuum model for weakly disordered Peierls chains is given by,

$$H[\Delta_{lat}(x),\eta(x)] \;=\; H_{el}[\Delta_{lat}(x),\eta(x)] \;+\; E_{lat}[\Delta_{lat}(x)] \;+\; H_{res}\;.\tag{2.30}$$

Here, the first term is the kinetic energy of the electrons including its dependence on the lattice Eq. (2.23). The second term in Eq. (2.30) is the potential lattice energy Eq. (2.28). The third term, H_{res}, represents residual interactions, such as the Coulomb interaction between electrons in the chain or three-dimensional effects due to the interaction between neighboring chains.

In Sections 2.2 and 2.3, we consider two well-known models as limiting cases of our model Eq. (2.30). The first one is the Takayama—Lin-Liu—Maki (TLM) model, which describes a single Peierls chain in the absence of both electron-electron interactions and disorder [4]. As the second limiting case we consider the Fluctuating Gap Model (FGM) for a single Peierls chain. This model accounts for the disorder, whereas the lattice energy and the residual interactions are not treated explicitly [5, 6]. We come back to the residual interactions in Section 2.4, where we will discuss effects of electron correlations and interchain interactions on the lattice dimerization of the Peierls chain.

2.2   The Takayama—Lin-Liu—Maki Model

In the absence of disorder and residual interactions, the Hamiltonian Eq. (2.30) reduces to the Takayama—Lin-Liu—Maki (TLM) model [4], which is the continuum version of the Su—Schrieffer—Heeger (SSH) model [1]. Studying the TLM model provides a fundamental understanding of Peierls systems, as it allows one to calculate the properties of the system's ground state and of its topological excitations analytically. Explicitly, the Hamiltonian reads:

$$H_{TLM}[\Delta_{lat}(x)] \;=\; \sum_{\sigma}\int dx\,\Psi_{\sigma}^{\dagger}(x)\,\hat{h}'(x)\,\Psi_{\sigma}(x) \;+\; E_{lat}[\Delta_{lat}(x)]\;.\tag{2.31}$$

The first term describes the kinetic energy of the electrons in the chain, where

$$\hat{h}'(x) \;=\; \frac{v_{F}}{i}\,\sigma_3\,\frac{d}{dx} \;+\; \Delta_{lat}(x)\,\sigma_1\tag{2.32}$$

corresponds to Eq. (2.24) in the limit of vanishing disorder, $\eta(x) = 0$, and the Fermi velocity is given by $v_F = 2at_0$. We use again the spinor notation Eq. (2.22) to describe left- and right-moving electrons. The second term in Eq. (2.31) is the potential lattice energy,

$$E_{lat}[\Delta_{lat}(x)] \;=\; \frac{1}{\pi\lambda v_{F}}\int dx\,\Delta_{lat}(x)^2\;,\tag{2.33}$$

as given by Eq. (2.28) with the dimensionless electron-lattice coupling constant λ defined by Eq. (2.29).

As the kinetic energy of the electrons is a functional of the lattice configuration, the total ground state energy, $E_{TLM}[\Delta_{lat}(x)] = \langle 0|H_{TLM}[\Delta_{lat}(x)]|0\rangle$, has to be calculated for the electronic ground state $|0\rangle$ associated with a given lattice configuration $\Delta_{lat}(x)$. It follows that the variation of $E_{TLM}[\Delta_{lat}(x)]$ with

$$\frac{\delta E_{TLM}[\Delta_{lat}(x)]}{\delta \Delta_{lat}(x)} = 0 \tag{2.34}$$

results in a self-consistency condition.

Labelling the eigenstates of $\hat{h}'(x)$ by ν, we expand the electron spinor wave function $\Psi_\sigma(x)$ in terms of the operators $c_{\nu,\sigma}$. The operator $c_{\nu,\sigma}$ annihilates an electron with spin projection σ in the energy level ν:

$$\Psi_\sigma(x) = \left(\begin{array}{c} \psi_{R,\sigma}(x) \\ \psi_{L,\sigma}(x) \end{array} \right) = \sum_\nu \Phi_\nu(x)\, c_{\nu,\sigma} \, . \tag{2.35}$$

Here, the electronic field is represented in terms of the wave function amplitudes $u_\nu(x)$ and $v_\nu(x)$ by the spinor

$$\Phi_\nu(x) = \left(\begin{array}{c} u_\nu(x) \\ v_\nu(x) \end{array} \right) \, , \tag{2.36}$$

which is normalized according to

$$\int dx\, \Phi_\nu^\dagger(x) \Phi_{\nu'}(x) = \delta_{\nu,\nu'} \, . \tag{2.37}$$

The ground state energy of H_{TLM} then becomes

$$E_{TLM}[\Delta_{lat}(x)] = \sum_{\nu,\sigma}{}' \varepsilon_\nu + \frac{1}{\pi\lambda v_F} \int dx\, \Delta_{lat}(x)^2 \, , \tag{2.38}$$

where the prime denotes the summation over occupied one-electron levels and

$$\varepsilon_\nu = \int dx\, \Phi_\nu^\dagger(x)\, \hat{h}'(x)\, \Phi_\nu(x) \tag{2.39}$$

is the energy of the ν'th electron level. The latter depends on $\Delta_{lat}(x)$.

We note that the spectrum of the single electron states of the TLM model is symmetric around energy zero, i.e., any energy level ε_ν will appear simultaneously with a level $-\varepsilon_\nu$ (except for $\varepsilon_\nu = 0$). This property follows from the charge conjugation symmetry of H_{TLM}, which states that for an eigenstate $\Phi_\nu(x)$ of $\hat{h}'(x)$ with energy ε_ν, satisfying

$$\hat{h}'(x)\, \Phi_\nu(x) = \left(\frac{v_F}{i}\, \sigma_3\, \frac{d}{dx} + \Delta_{lat}(x)\, \sigma_1 \right) \Phi_\nu(x) = \varepsilon_\nu\, \Phi_\nu(x) \, , \tag{2.40}$$

there exists an eigenstate $\sigma_2 \Phi_\nu(x)$ of $\hat{h}'(x)$ with energy $-\varepsilon_\nu$,

$$\hat{h}'(x) \left[\sigma_2 \Phi_\nu(x)\right] = -\varepsilon_\nu \left[\sigma_2 \Phi_\nu(x)\right] \, . \tag{2.41}$$

We thus represent $\Phi_\nu(x)$ in terms of the normalized eigenfunctions $|\pm\rangle$ of the Pauli matrix σ_2,

$$\Phi_\nu(x) \;=\; \frac{1}{\sqrt{2}}\left[f_\nu^+(x)\,|+\rangle \;+\; f_\nu^-(x)\,|-\rangle \right] \;, \tag{2.42}$$

where we introduced two new functions $f_\nu^\pm(x)$, while

$$|\pm\rangle \;=\; \frac{1}{\sqrt{2}}\begin{pmatrix} 1 \\ \pm i \end{pmatrix} \;, \tag{2.43}$$

which fulfill $\sigma_2|\pm\rangle = \pm|\pm\rangle$. Using Eq. (2.36), the wave function amplitudes are given by

$$u_\nu(x) \;=\; \frac{1}{2}\big(f_\nu^+(x) + f_\nu^-(x)\big) \quad \text{and} \quad v_\nu(x) \;=\; \frac{i}{2}\big(f_\nu^+(x) - f_\nu^-(x)\big) \;. \tag{2.44}$$

We calculate the functions $f_\nu^+(x)$ and $f_\nu^-(x)$ for a particular lattice distortion $\Delta_{lat}(x)$ by a variation of the ground state energy Eq. (2.38) with respect to $\Phi_\nu^\dagger$ under the normalization condition Eq. (2.37). This procedure leads to the so-called Bogoliubov—de Gennes equations which can be written in the compact form

$$\mathcal{D}^\pm f_\nu^\pm(x) \;=\; \varepsilon_\nu f_\nu^\mp(x) \;, \tag{2.45}$$

with the differential operator

$$\mathcal{D}^\pm \;=\; \frac{v_F}{i}\frac{d}{dx} \pm i\,\Delta_{lat}(x) \;. \tag{2.46}$$

For a given lattice distortion $\Delta_{lat}(x)$, the spectrum ε_ν and the functions $f_\nu^\pm(x)$ can, in principle, be found by solving Eq. (2.45) together with the normalization condition Eq. (2.37), which translates into

$$\frac{1}{2}\int dx \left(|f_\nu^+(x)|^2 \;+\; |f_\nu^-(x)|^2 \right) \;=\; 1 \;. \tag{2.47}$$

In addition, we obtain an eigenvalue equation by applying the differential operator $\mathcal{D}^\mp$ from the left in Eq. (2.45),

$$\left(\mathcal{H}^\pm \;-\; \varepsilon_\nu^2 \right) f_\nu^\pm(x) \;=\; 0 \;, \tag{2.48}$$

where $f_\nu^\pm(x)$ represents an eigenfunction corresponding to the non-negative eigenvalue ε_ν^2 of the operator

$$\mathcal{H}^\pm \;\equiv\; \mathcal{D}^\mp\mathcal{D}^\pm \;=\; -v_F^2\frac{d^2}{dx^2} \;+\; \Delta_{lat}(x)^2 \pm v_F\frac{\partial\Delta_{lat}(x)}{\partial x} \;. \tag{2.49}$$

Once we determined $f_\nu^\pm(x)$ as a function of $\Delta_{lat}(x)$, the optimal lattice distortion is found from the self-consistency condition

$$\Delta_{lat}(x) \;=\; -i\frac{\pi\lambda v_F}{4}\sum_{\nu,\sigma}{}' \big(f_\nu^-(x)^* f_\nu^+(x) \;-\; f_\nu^+(x)^* f_\nu^-(x)\big) \;, \tag{2.50}$$

which follows from Eqs. (2.34), (2.38) and (2.39).

In Section 2.2.1 we consider the ground state of a Peierls chain for which the Peierls order parameter is a constant, $\Delta_{lat}(x) = \Delta_{lat}$. We calculate the total energy of the Peierls chain as a function of Δ_{lat} and find the optimal value $\Delta_{lat} = \Delta_0$ from the self-consistency condition Eq. (2.50). Next, in Section 2.2.2, we consider locally stable inhomogeneous solutions of the order parameter $\Delta_{lat}(x)$, such as the soliton, and discuss several properties of these topological excitations.
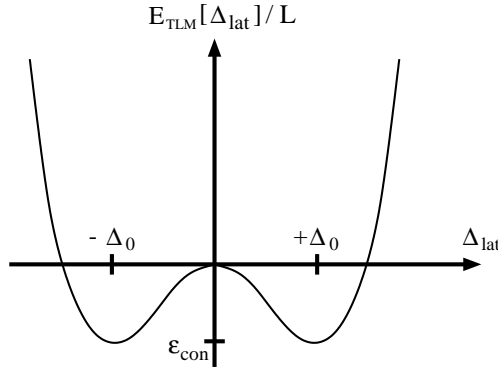
Figure 2-3: *The total energy $E_{TLM}[\Delta_{lat}]/L$ is an even function of the homogeneous lattice distortion Δ_{lat}. The two degenerate minima at $\Delta_{lat} = \pm\Delta_0$ correspond to the two possible ground state bond alternation patterns in a half-filled chain (see Figure 2-4).*

2.2.1 Ground state: Peierls distortion

A constant Peierls order parameter, $\Delta_{lat}(x) = \Delta_{lat}$, corresponds to a bond-length alternation in the one-dimensional lattice of a half-filled system. We mentioned already in Section 2.1, that $\Delta_{lat} = 4\alpha u$ for a bond-length alternation with atomic displacement $u_n = -(-1)^n u$ of the n'th atom, where α is the electron-lattice coupling constant (see Eqs. (2.16) and (2.17)). In this section, we restrict our considerations to a chain with an even number of sites and impose periodic boundary conditions ($u_{N+1} = u_1$) to calculate the optimal value $\Delta_{lat} = \Delta_0$ which minimizes the total energy $E_{TLM}[\Delta_{lat}]$.

We start by noting that the operators Eq. (2.49) take a simple form in the case $\Delta_{lat}(x) = \Delta_{lat}$, namely

$$\mathcal{H}_0 \equiv \mathcal{H}^\pm = -v_F^2 \frac{d^2}{dx^2} + \Delta_{lat}^2 \,, \tag{2.51}$$

and the corresponding eigenvalue equation (2.48) is solved by plane waves $f_\kappa^\pm(x) = A_\kappa^\pm e^{i\kappa x}$. We recover the single electron spectrum Eq. (2.19), where $\varepsilon_\kappa = s|\varepsilon_\kappa|$ with $s = \pm 1$ and

$$|\varepsilon_\kappa| = \sqrt{v_F^2 \kappa^2 + \Delta_{lat}^2} \tag{2.52}$$

describes the valence ($s = -1$) and conduction ($s = +1$) band close to the Fermi points. These bands are separated by an energy gap $2\Delta_{lat}$. The differential equations (2.45) together with the normalization condition Eq. (2.47) have the solutions

$$f_\kappa^-(x) = \frac{\exp{(i\,\kappa\,x)}}{\sqrt{L}} \quad \text{and} \quad f_\kappa^+(x) = \frac{\exp{(i\,\kappa\,x)}}{\sqrt{L}} \frac{v_F \kappa - i\Delta_{lat}}{\varepsilon_\kappa} \tag{2.53}$$

for a chain of length L. It is now straightforward to calculate the total energy Eq. (2.38) of the TLM model, if the wave function amplitudes Eq. (2.44) are expressed in terms of $f_\kappa^\pm(x)$ as given by Eq. (2.53). We find
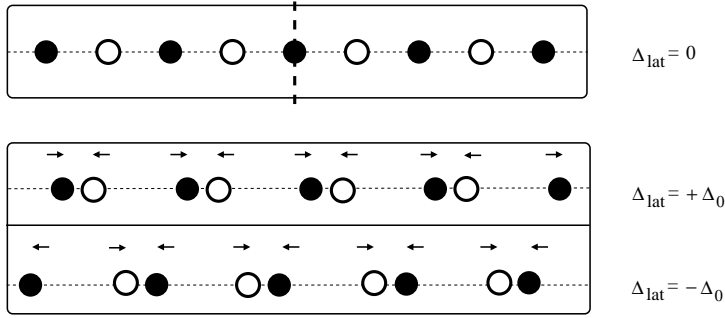
Figure 2-4: *A chain of equidistant even (●) and odd (○) sites of atoms is symmetric under a reflection on a plane perpendicular to the chain direction at any site. This is indicated by the vertical dashed line. The two possible bond alternation patterns originate from a shift of either the even sites (●) to the right and the odd (○) sites to the left or vice versa, and are characterized by, respectively, $\Delta_{lat} = +\Delta_0$ or $\Delta_{lat} = -\Delta_0$. The reflection symmetry is seen to be broken in the dimerized lattice.*

$$E_{TLM}[\Delta_{lat}] \ = \ E_{TLM}[0] - L \, \frac{\Delta_{lat}^2}{2\pi v_F} \left[1 - 2\ln \left| \frac{\Delta_{lat}}{W} \right| \right] + L \, \frac{\Delta_{lat}^2}{\pi\lambda v_F} \ , \tag{2.54}$$

where $W = 2v_F/a$ is the electron band width and λ is the dimensionless electron-lattice coupling constant defined by Eq. (2.29). Figure 2-3 is a schematic plot of Eq. (2.54). It is seen that $E_{TLM}[\Delta_{lat}]$ is an even function of Δ_{lat} with two degenerate minima at $\Delta_{lat} = \pm\Delta_0$. The system's gain in the electronic energy due to the lattice dimerization, which is given by the second term in Eq. (2.54), is larger than the loss in the lattice energy which is proportional to Δ_{lat}^2 (third term in Eq. (2.54)). The doubly degenerate ground state corresponds to the two possible sequences in the bond alternation of the lattice configuration (...–long–short–long–short–... for $\Delta_{lat} = +\Delta_0$ and ...–short–long–short–long–... for $\Delta_{lat} = -\Delta_0$). In the absence of the lattice dimerization, $\Delta_{lat} = 0$, the system has a reflection symmetry with respect to a plane perpendicular to the chain direction at any atomic site in the chain. This is indicated in Figure 2-4, which also shows that this symmetry is broken in a dimerized lattice, since the lattice dimerization changes under a reflection from $\Delta_{lat} = \pm\Delta_0$ into $\Delta_{lat} = \mp\Delta_0$.

The optimal value of the Peierls order parameter, Δ_0, is obtained from a minimization of Eq. (2.54) with respect to Δ_{lat}. We find the so-called gap equation

$$\Delta_0 \ = \ W \exp\left(-\frac{1}{\lambda} \right) \ , \tag{2.55}$$

which is a function of the dimensionless electron-lattice coupling λ. The gap equation predicts a nonzero value $2\Delta_0$ of the energy gap at the Fermi points for any finite value of the electron-lattice coupling constant α. We briefly note that the gap equation (2.55) also follows directly from the self-consistency condition Eq. (2.50), which becomes

$$\Delta_0 \ = \ \lambda \, v_F \int_{-\frac{W}{2v_F}}^{0} d\kappa \, \frac{\Delta_0}{|\varepsilon_\kappa|} \tag{2.56}$$

in terms of the expressions Eq. (2.53) for $f_\kappa^\pm(x)$. The condensation energy per unit length is calculated from Eq. (2.54) with Eq. (2.55) and is given by

$$\varepsilon_{con} = \left(E_{TLM}[\pm\Delta_0] - E_{TLM}[0]\right)/L \approx -\frac{\Delta_0}{2\pi\xi_0} \ . \tag{2.57}$$

Here, we introduced the characteristic length of the continuum model,

$$\xi_0 = \frac{v_F}{\Delta_0} \ , \tag{2.58}$$

which has a concrete meaning, as it corresponds to electron momentum $\kappa_0 = \xi_0^{-1}$ of the relevant electron states. In the derivation of the continuum model (see Section 2.1), this deviation is assumed to be small, $\kappa_0 \ll a^{-1}$, to justify the linearization of the electronic spectrum Eq. (2.52) close to the Fermi points. It follows from the definition of ξ_0, that this assumption is equivalent to the condition that the Peierls gap is small compared to the electron band width, $2\Delta_0/W \ll 1$ (weak-coupling limit).

It should be mentioned that it has been rigorously proven, that the dimerized lattice is the true ground state configuration of the half-filled system and that any other lattice configuration, including additional symmetry breaking, is higher in energy [7, 8]. A dimerization of the lattice in *trans*-polyacetylene has been confirmed by X-ray scattering and NMR experiments with an atomic displacement of the order $u/a \sim 3\%$ [9, 10].

We conclude this section with a brief discussion of the Peierls transition temperature T_c at which the Peierls order parameter vanishes. The optimal value of the Peierls order parameter as a function of the temperature, $\Delta_0(T)$, is determined by the self-consistency condition

$$\Delta_0(T) = \lambda v_F \int_{-\frac{W}{2v_F}}^0 d\kappa \, \frac{\Delta_0(T)}{|\varepsilon_\kappa|} \, \tanh\left(\frac{|\varepsilon_\kappa|}{2T}\right) \tag{2.59}$$

within the mean-field approximation [11]. Here, $\pm|\varepsilon_\kappa|$ denotes again the single electron spectrum Eq. (2.52). The $\tanh$-term in the integrand accounts for the thermal occupation of electron states according to the Fermi distribution $n_F(\pm|\varepsilon_\kappa|)$ and is obtained within linear response theory, $\tanh(|\varepsilon_\kappa|/(2T)) = n_F(-|\varepsilon_\kappa|) - n_F(+|\varepsilon_\kappa|)$. At zero temperature Eq. (2.59) reduces to Eq. (2.56) and the Peierls order parameter $\Delta_0(0)$ equals Δ_0, while it is decreased, $\Delta_0(T) < \Delta_0$, for temperatures $T > 0$. The Peierls transition temperature T_c is determined from Eq. (2.59) under the condition $\Delta_0(T_c) = 0$ resulting in the mean-field expression

$$T_c = \frac{\gamma}{\pi} W \exp\left(-\frac{1}{\lambda}\right) \ , \tag{2.60}$$

where $\gamma = 1.781072...$ is the exponential of Euler's constant.

2.2.2   Inhomogeneous solutions of the Peierls order parameter

If the Peierls order parameter $\Delta_{lat}(x)$ varies along the chain as a function of x, it is, in general, difficult to solve the Bogoliubov—de Gennes equations (2.45) for the functions $f_\nu^\pm(x)$ analytically and to calculate properties of the corresponding lattice configuration. However, it

is possible to find an analytical solution for $f_\nu^\pm(x)$, if $\Delta_{lat}(x)$ satisfies the differential equation

$$\Delta_{lat}(x)^2 + v_F \frac{\partial \Delta_{lat}(x)}{\partial x} = \Delta_{lat}^2 \,, \tag{2.61}$$

where Δ_{lat} is assumed to have a constant value. This is evident from the fact that in this case the operator $\mathcal{H}^+$ reduces again to $\mathcal{H}_0$ as given by Eq. (2.51),

$$\mathcal{H}^+ = -v_F^2 \frac{d^2}{dx^2} + \Delta_{lat}^2 \,. \tag{2.62}$$

It thus follows that the eigenvalue equation (2.48), $\mathcal{H}^+ f_\nu^+(x) = \varepsilon_\nu^2 f_\nu^+(x)$, can again be solved by a plane wave ansatz,

$$f_\kappa^+(x) = B_\kappa^+ \exp(i\,\kappa\,x) \,. \tag{2.63}$$

Therefore, the single electron dispersion is immediately found to be the same as for a homogeneous Peierls order parameter $(\Delta_{lat}(x) = \Delta_{lat})$, where $\varepsilon_\kappa = s|\varepsilon_\kappa|$ with $|\varepsilon_\kappa|$ as given by Eq. (2.52) and $s = \pm 1$ refers to the valence and conduction band which are separated by an energy gap $2\Delta_{lat}$. In order to find $f_\kappa^-(x)$, we apply Eq. (2.45) and obtain the solution

$$f_\kappa^-(x) = f_\kappa^+(x) \frac{v_F \kappa + i\,\Delta_{lat}(x)}{\varepsilon_\kappa} \tag{2.64}$$

for non-zero $\varepsilon_\nu = \varepsilon_\kappa$. For $\varepsilon_\nu = 0$, however, it follows from Eq. (2.45) that

$$f^+(x) = 0 \quad \text{and} \quad f^-(x) = B^- \exp\left\{ -\frac{1}{v_F} \int dx \Delta_{lat}(x) \right\} \tag{2.65}$$

with normalization constant B^-. The solution Eq. (2.65) for $\varepsilon_\nu = 0$ represents an isolated midgap state, which depends on the particular lattice configuration $\Delta_{lat}(x)$. We finally solve the differential equation (2.61) for the lattice configuration $\Delta_{lat}(x)$ and obtain the kink solution $\Delta_{lat}(x) = \Delta_s(x)$ with

$$\Delta_s(x) = \Delta_0 \tanh\left(\frac{x}{\xi_0} \right) \,. \tag{2.66}$$

This lattice configuration describes a change of the sign in the lattice dimerization from $\Delta_s(-L/2) = -\Delta_0$ to $\Delta_s(+L/2) = +\Delta_0$ that takes place around $x = 0$ over a region of the size $2\xi_0$. This kink solution, which is often called a 'soliton', is a domain wall that interpolates between the two degenerate ground state lattice configurations that are characterized by $\Delta_{lat}(x) = \pm\Delta_0$. The soliton is depicted in Figure 2-5 together with the antisoliton, $\Delta_{lat}(x) = -\Delta_s(x)$, which is a related inhomogeneous solution of the Peierls order parameter that follows from the symmetry of the Bogoliubov—de Gennes equations (2.45).

We note that topological constraints, as given by the number of sites and the boundary conditions, are necessary prerequisites for the existence of solitons. The ground state of the Peierls chain corresponds to a uniformly dimerized lattice, where the atomic displacement u_n of the n'th atom is given by Eq. (2.16). It follows with Eq. (2.17), that the slowly varying part of the lattice dimerization is given by $\Delta_{lat}(x)$ with boundary conditions

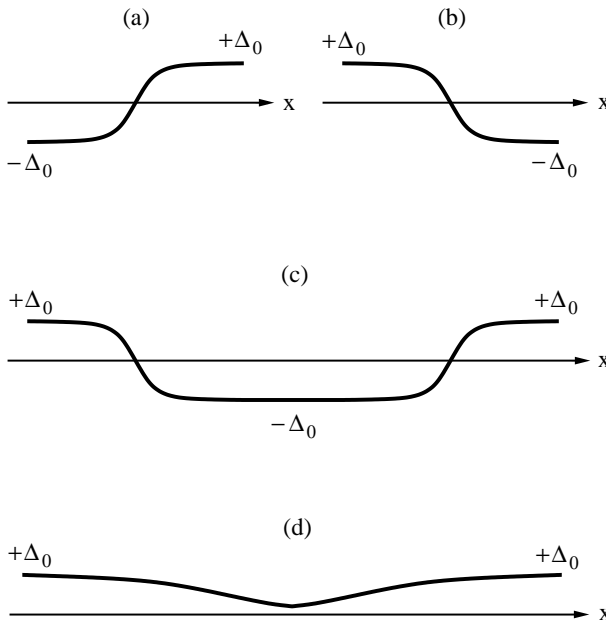$$\Delta_{lat}(x + L) = b\,(-1)^N \Delta_{lat}(x) \,. \tag{2.67}$$

Figure 2-5: *Several inhomogeneous solutions of the Peierls order parameter* $\Delta_{lat}(x)$*: (a) soliton, (b) antisoliton, (c) soliton-antisoliton pair, and (d) polaron. See the text for details.*

Here, we have $b = +1$ if periodic and $b = -1$ if antiperiodic boundary conditions are imposed for the atomic displacements u_n in a chain with $N = L/a$ sites. Thus, periodic boundary conditions require a soliton to be present in a chain with an odd number of sites, whereas in a chain with an even number of sites a soliton is required for antiperiodic boundary conditions.

In what follows, we discuss several properties of the soliton, such as the creation energy, the mass, and the exotic spin-charge relations. To calculate the soliton creation energy,

$$\mu = \Delta E_{el} + \Delta E_{lat} , \tag{2.68}$$

we consider a system that contains a single soliton, $\Delta_{lat}(x) = \Delta_s(x)$, by imposing periodic boundary conditions in a chain with an odd number of sites. We calculate the change in the electronic energy, ΔE_{el}, and in the lattice energy, ΔE_{lat}, compared to the same chain with antiperiodic boundary conditions for which the lattice is uniformly dimerized, $\Delta_{lat}(x) = \Delta_0$. The latter case is comparable to a chain with an even number of sites and periodic boundary conditions which has been discussed in Section 2.2.1.

Here, we start with the normalization of $f_\nu^{\pm}(x)$ according to Eq. (2.47) and obtain from Eqs. (2.63)-(2.65), that

$$f_\kappa^+(x) = \frac{\exp\left(i\,\kappa\,x\right)}{\sqrt{L - \xi_0 \Delta_0^2/\varepsilon_\kappa^2}} \quad \text{and} \quad f_\kappa^-(x) = \frac{\exp\left(i\,\kappa\,x\right)}{\sqrt{L - \xi_0 \Delta_0^2/\varepsilon_\kappa^2}}\,\frac{v_F\kappa + i\Delta_s(x)}{\varepsilon_\kappa} \tag{2.69}$$

with $\varepsilon_\kappa = \pm\sqrt{v_F^2 \kappa^2 + \Delta_0^2}$, while

$$f^+(x) \;=\; 0 \quad \text{and} \quad f^-(x) \;=\; \frac{1}{\sqrt{\xi_0}}\,\frac{1}{\cosh(x/\xi_0)} \tag{2.70}$$

for the midgap state with $\varepsilon_\nu = 0$. The boundary conditions for the fields of the right- and left-moving electrons follow from Eq. (2.21):

$$\begin{aligned}
\psi_{R,\sigma}(x+L) &= b\,(-i)^N\,\psi_{R,\sigma}(x) \\
\psi_{L,\sigma}(x+L) &= b\,(+i)^N\,\psi_{L,\sigma}(x)\,,
\end{aligned} \tag{2.71}$$

where $b = +1$ ($b = -1$) refers again to periodic (antiperiodic) boundary conditions for the electrons. Using Eqs. (2.36) and (2.44) we can translate Eq. (2.71) into

$$f_\nu^\pm\,(L/2) \;=\; -\,b\,(+i)^N\,f_\nu^\mp\,(-L/2)\,. \tag{2.72}$$

For the chain with an odd number of sites and periodic boundary conditions, we choose $f_\kappa^\pm(L/2) = -if_\kappa^\mp(-L/2)$. It then follows from Eq. (2.69), that the electron momentum κ is given by

$$\kappa L \;=\; \begin{cases} 2n_s\pi + \tan^{-1}(\kappa\xi_0) & \text{for } \varepsilon_\kappa > 0 \\[2ex] (2n_s+1)\pi + \tan^{-1}(\kappa\xi_0) & \text{for } \varepsilon_\kappa < 0 \end{cases} \tag{2.73}$$

where the integer n_s counts the number of states. Compared to the density of states for the chain with antiperiodic boundary conditions and a uniformly dimerized lattice, $dn/d\kappa = L/(2\pi)$, the density of states in the present case is found to be modified:

$$\frac{dn_s}{d\kappa} \;=\; \frac{dn}{d\kappa}\left(1 - \frac{\xi_0}{L}\,\frac{\Delta_0^2}{\varepsilon_\kappa^2}\right)\,. \tag{2.74}$$

This modification is due to the presence of the soliton in the lattice dimerization which affects the whole electron spectrum. As a consequence of the system's charge conjugation symmetry, the midgap state Eq. (2.70) requires that the number of states change by $\Delta N = -1/2$ per band. In the continuum model this is taken into account by choosing a cut-off Λ_s which is slightly different from $\Lambda = W/(2v_F)$ for the uniformly dimerized lattice. From the condition

$$\Delta N \;=\; 2\int_0^{\Lambda_s} d\kappa \frac{dn_s}{d\kappa} - 2\int_0^{\Lambda} d\kappa \frac{dn}{d\kappa} \;=\; -\frac{1}{2}\,, \tag{2.75}$$

one obtains $\Lambda_s \approx \Lambda - (\Lambda\xi_0 L)^{-1}$. We are now able to calculate the amount by which the electronic energy is increased in the presence of the soliton:

$$\Delta E_{el} \;=\; -4\int_{-\Lambda_s}^{0} d\kappa \frac{dn_s}{d\kappa}|\varepsilon_\kappa| + 4\int_{-\Lambda}^{0} d\kappa \frac{dn}{d\kappa}|\varepsilon_\kappa| \;\approx\; \frac{2\Delta_0}{\pi}\left[1 + v_F\int_{-\Lambda_s}^{0} d\kappa \frac{1}{|\varepsilon_\kappa|}\right]\,. \tag{2.76}$$

This loss in the electron condensation energy is partly recovered by a decrease of the lattice energy which is given by

$$\Delta E_{lat} \;=\; \frac{1}{\pi\lambda v_F}\int_{-L/2}^{L/2} dx\,\left(\Delta_s(x)^2 - \Delta_0^2\right) \;\approx\; -\frac{2\Delta_0}{\pi}\,\frac{1}{\lambda}\,. \tag{2.77}$$

It follows from the gap equation (2.55) that the lattice energy ΔE_{lat} and the second term in the square brackets of Eq. (2.76) add to zero if we neglect minor corrections of the order $(\Delta_0/W)^2$. In other words, since the self-consistency condition Eq. (2.50) does not depend on the occupation of the midgap state Eq. (2.70), we recover the optimal value $\Delta_{lat} = \Delta_0$ for a completely filled valence and an empty conduction band in the chain with $\Delta_{lat}(x) = \Delta_s(x)$. This completes the proof that the (anti-) soliton provides an inhomogeneous solution of the TLM model. Thus, the second term in the square brackets of Eq. (2.76) and ΔE_{lat} add to zero and we obtain the creation energy of the soliton to be [4]:

$$\mu = \Delta E_{el} + \Delta E_{lat} \approx \frac{2\Delta_0}{\pi} . \tag{2.78}$$

From the experimental value of the charge gap in *trans*-polyacetylene, $E_g = 2\Delta_0 \approx 1.8$ eV [12], the soliton creation energy is estimated to be $\mu \sim 0.5$ eV.

Next, we estimate the soliton mass M_s from its kinetic energy, E_s, according to

$$E_s = \frac{1}{2} M_s v_s^2 \sim \frac{1}{2} M_{CH} \int_{-L/2}^{L/2} \frac{dx}{2a} \left(\frac{1}{4\alpha} \frac{d}{dt} \Delta_s(x - v_s t) \right)^2 , \tag{2.79}$$

where v_s is the velocity of the (slowly) moving soliton $\Delta_s(x - v_s t)$ and M_{CH} is the mass of a carbon-hydrogen group in *trans*-polyacetyelene. Typical parameters for *trans*-polyacetylene [1] yield

$$M_s \sim M_{CH} \left(\frac{u_0}{a} \right)^2 \frac{a}{\xi_0} \sim 6\, m_e \tag{2.80}$$

where m_e is the electron mass. The smallness of M_s is a consequence of the large soliton extent, $2\xi_0/a \sim 14$, and the small atomic displacements $u_0/a \sim 0.03$, so that a carbon-hydrogen group gains little kinetic energy as the soliton passes. Its low mass implies that the soliton has a high mobility. However, the soliton can move freely along the chain only within the continuum TLM model. In the discrete SSH model a moving soliton has to overcome the Peierls-Nabarro barrier which is associated with the lattice discreteness and has a height of about 30 K [13]. Moreover, disorder effects will increase this pinning energy and further hinder the free translation of the soliton.

We now turn to a discussion of the soliton's exotic spin-charge relations. These relations follow from the charge conjugation symmetry which results in an equal contribution of the valence and conduction band to the density $\rho_\sigma(x)$ of electrons with spin σ, and from the existence of a midgap state,

$$\Phi_0(x) = \frac{1}{\sqrt{2\xi_0}} \frac{1}{\cosh(x/\xi_0)} |-\rangle . \tag{2.81}$$

Using the completeness relation of the one-particle eigenstates, the density of spin σ electrons becomes

$$\rho_\sigma(x) = \frac{1}{2a} + \left(N_\sigma - \frac{1}{2} \right) |\Phi_0(x)|^2 , \tag{2.82}$$

where N_σ equals unity if the midgap state is occupied by an electron with spin σ and zero otherwise. As can be seen in Figure 2-6, $|\Phi_0(x)|^2$ is exponentially confined to a region of width
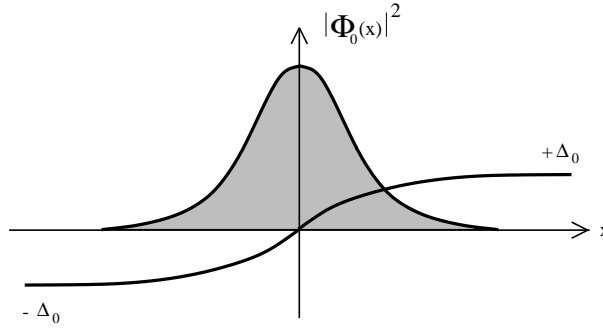
Figure 2-6: *The amplitude of the midgap state, $|\Phi_0(x)|^2$, is exponentially confined to a region of width $2\xi_0$ around the soliton position $x = 0$. The same holds for the profile of the spin density Eq. (2.83) in the case of a neutral soliton, $|s(x)| = |\Phi_0(x)|^2/2$, and the profile of the charge density Eq. (2.84) in the case of a charged soliton with spin zero, $|q(x)| = |\Phi_0(x)|^2/e$.*

$2\xi_0$ around the soliton position and the same holds for the profile of $\rho_\sigma(x)$. The total spin associated with the soliton is then given by $S = \int dx s(x)$, where the spin density is given by

$$s(x) \;=\; \frac{1}{2}\left[\rho_\uparrow(x) - \rho_\downarrow(x)\right] \;=\; \frac{1}{2}\left[N_\uparrow - N_\downarrow\right]|\Phi_0(x)|^2 \;, \tag{2.83}$$

and we otain $S = \frac{1}{2}[N_\uparrow - N_\downarrow]$. Similarly, the charge associated with the soliton is calculated from $Q = \int dx q(x)$. The charge density $q(x)$, which accounts also for the background charge that makes the system neutral in the absence of a soliton, is given by

$$q(x) \;=\; -e\sum_\sigma\left[\rho_\sigma(x) - \frac{1}{2a}\right] \;=\; -e\left[N_\uparrow + N_\downarrow - 1\right]|\Phi_0(x)|^2 \tag{2.84}$$

where $-e$ is electron charge, so that the soliton charge becomes $Q = -e[N_\uparrow + N_\downarrow - 1]$. It thus follows in the case of a singly occupied midgap state (e.g. $N_\uparrow = 1$ and $N_\downarrow = 0$), that the soliton has spin $S = 1/2$ and is charge-neutral, $Q = 0$. On the other hand, adding to the neutral system one electron ($N_\uparrow = N_\downarrow = 1$) or one hole ($N_\uparrow = N_\downarrow = 0$), a charged soliton with $Q = \mp e$ and spin $S = 0$ is created [13, 14]. These spin-charge relations are probably the most surprising property of the soliton in *trans*-polyacetylene because they are reversed compared to the spin-charge relations of the constituents of the theory.

It is rather unlikely that a neutral soliton is thermally excited in *trans*-polyacetylene because of its large creation energy $\mu \sim 6000$ K. The reason why, nevertheless, the domain walls may play a role is the defected nature of this polymer. In the processes of polymerization and isomerization various types of defects are induced which interrupt the conjugation. The conjugation length of chain segments in the (partially) crystalline phase may be still much larger than the characteristic length ξ_0, however, the chain segments will contain even or odd numbers of carbon-hydrogen groups. In general, depending on the chemical nature of a chain end, a surface energy may favor one bond alternation phase over the other and it has been found in the case of *trans*-polyacteylene that a finite chain has a strong preference to end with a double bond [16]. Therefore, it has been concluded that all chains with an odd number of
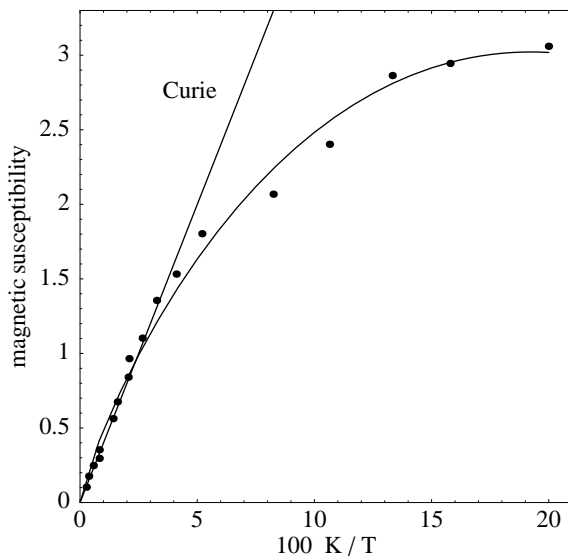
Figure 2-7: *Experimental results (dots) for the magnetic susceptibility as a function of inverse temperature* T *in a sample of undoped Durham trans-polyactylene according to Ref. [15]. At low temperatures,* T < 30 *K, the magnetic susceptibility is clearly seen to deviate from the Curie behavior. The solid curves are a guide to the eye.*

carbon-hydrogen groups contain necessarily a domain wall in the inner part. In fact, it seems possible to explain the peculiar behavior of the magnetic susceptibiliy of *trans*-polyacetylene by the exotic spin-charge relation of neutral solitons [13]. The Curie susceptibility of undoped *trans*-polyacetylene can be attributed to the spin of these domain walls. Upon doping the system with electrons, the magnetic susceptibility is found to be reduced and this can be readily understood within the soliton picture, because the added electrons will occupy these midgap states resulting into excitations which are charged but do not carry spin. At low temperatures, T < 30 K, the magnetic susceptibility of undoped *trans*-polyacetylene is found to clearly deviate from the Curie behavior. This can be seen in Figure 2-7 which shows the magnetic susceptibility as a function of inverse temperature in a sample of Durham *trans*-polyactylene [15]. We propose an explanation for this behavior in Chapter 5, where we study the effect of interchain interactions on the disorder-induced neutral solitons.

A single soliton does not exist in the lattice of a chain with an even number of sites if periodic boundary conditions are imposed. Instead, the topological constraints require an excitation to change the sign of the lattice dimerization at least two times along the chain. A soliton-antisoliton pair $\Delta_p(x)$ which is shown in Figure 2-5 (c) fulfills this condition. The lattice dimerization $\Delta_p(x)$ for a pair of size R is given by

$$\Delta_p(x) \; = \; \Delta_0 \, - \, \Delta_0 \, k_0 \, \xi_0 \left[\tanh\left(k_0 \left(x + \frac{R}{2} \right) \right) \, - \, \tanh\left(k_0 \left(x - \frac{R}{2} \right) \right) \right] \, , \qquad (2.85)$$

where the parameter k_0 depends crucially on the filling of the electronic levels [17]. It follows from the self-consistency condition Eq. (2.50) that k_0 is related to the characteristic length ξ_0

and the pair size R by the equation

$$k_0 \xi_0 \; = \; \tanh(k_0 R) \,. \tag{2.86}$$

The topological excitation Eq. (2.85) changes the electronic spectrum by producing two local-ized intragap states accompanied by a modification of the density of band states. The states in the gap are the symmetric and antisymmetric superpositions of midgap states Eq. (2.81) localized near the soliton and the antisoliton:

$$\Phi_\pm(x) \; = \; \frac{1}{\sqrt{2}} \left[\frac{\sqrt{k_0/2}}{\cosh(k_0(x - R/2))} \, |-\rangle \pm \frac{\sqrt{k_0/2}}{\cosh(k_0(x + R/2))} \, |+\rangle \right] \tag{2.87}$$

with energies

$$\pm \varepsilon(R) \; = \; \pm \frac{\Delta_0}{\cosh(k_0 R)} \,. \tag{2.88}$$

For vanishing pair size, $R \to 0$, the perfectly dimerized system is recovered where the bonding state becomes the top of the valence band and the antibonding state the bottom of the conduction band, $\pm \varepsilon(R) \to \pm \Delta_0$. On the other hand, for a well-separated soliton-antisoliton pair, $R \gg \xi_0$, the splitting between the two energy levels $\pm \varepsilon(R)$ is exponentially small. Since the corresponding bound state wave functions fall off exponentially, so does the hybridization and it follows from Eq. (2.86) that $k_0 \simeq 1/\xi_0$ in this limit.

Clearly, the energy associated with a soliton-antisoliton pair of size R depends on the occupancy $n_\pm$ of the gap states $\pm \varepsilon(R)$. Because of the spin degeneracy $n_\pm$ can be equal to $0, 1$ or 2. For the neutral chain the occupancy is $n_- = 2$, $n_+ = 0$ and beside the perfectly dimerized state the only stable solution is the well separated soliton-antisoliton pair ($R \gg \xi_0$) with creation energy 2μ. The electronic ground state of the chain in the presence of a single added charge, where the occupation is $n_- = 2$, $n_+ = 1$ for an electron or $n_- = 1$, $n_+ = 0$ for a hole, results in a polaron. This is a nontopological excitation, as the sign of the lattice dimerization does not change and the stable solution $\Delta_p(x)$ describes a local dip at $x = 0$ which is extended over $R = \sqrt{2} \ln(1 + \sqrt{2})\xi_0$. The polaron solution is plotted in Figure 2-5 (d) and its creation energy is found to be $\mu_p = \sqrt{2}\mu \approx 0.9\Delta_0$ and is, thus, less than Δ_0 [17]. However, twice the soliton creation energy is still less than $2\mu_p$ meaning that solitons are the lowest-energy charge excitations in the TLM model.

To conclude this section, we summarize several aspects of the TLM model in Figure 2-8, where the one-electron density of states $\rho(E)$ is plotted as a function of the energy E for three different lattice configurations [18]. The symmetry $\rho(E) = \rho(-E)$ reflects the charge conjugation symmetry of the TLM model and the density of states for a uniformly dimerized lattice displays the Peierls gap for energies $|E| < \Delta_0$ where $\rho(|E| < \Delta_0) = 0$. The density of states diverges at the top of the valence band and the bottom of the conduction band as the electron velocity becomes zero at $|E| = \Delta_0$. The presence of a soliton in an otherwise uniformly dimerized chain results in a localized electronic state at $E = 0$, while the valence and conduction band are each depleted by one-half of a state. Similarly, for a soliton-antisoliton pair the density of states contains two localized states at energies $\pm \varepsilon$ accompanied by a further reduction in the band states.
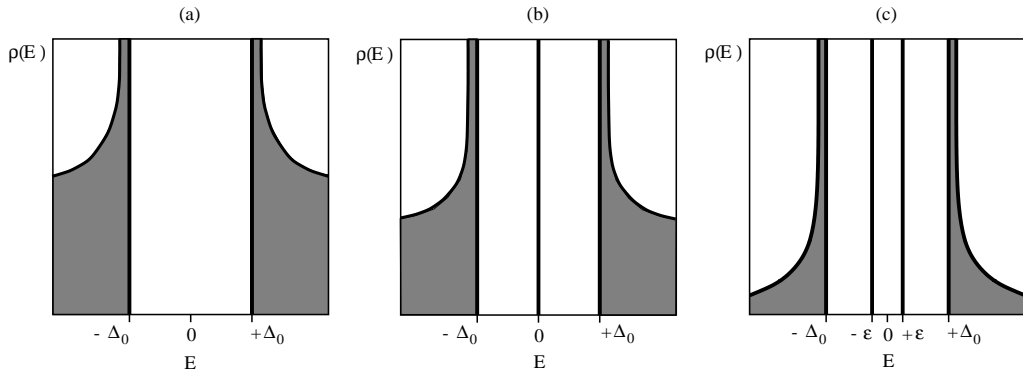
Figure 2-8: *Qualitative plot of the density of electron states $\rho(E)$ in the TLM model for three lattice configurations: (a) a uniformly dimerized chain, (b) a uniformly dimerized chain containing a soliton, and (c) a uniformly dimerized chain containing a soliton-antisoliton pair.*

Disorder is not taken into account in the TLM model. In practice, however, disorder is certainly present and will affect the properties of the Peierls chains resulting, for example, in a modified density of states. In the next section, we discuss the density of states in the Fluctuating Gap Model, which has been proposed to describe disorder effects in Peierls materials. An alternative model will be presented in Chapter 3.

2.3   The Fluctuating Gap Model

The Fluctuating Gap Model (FGM) describes the low-energy physics of electrons subject to a static disorder potential in a one-dimensional chain of atoms. The FGM has previously been applied to study the effect of disorder on the Peierls transition [5, 19], as well as the effect of quantum lattice fluctuations on the optical spectrum of Peierls materials [20, 21, 22], and has also been considered in the context of quasi-one-dimensional charge-transfer salts [6].

We introduced in Section 2.1 the continuum model Eq. (2.30) for weakly disordered Peierls chains. In the absence of residual interactions, $H_{res} = 0$, and neglecting the energy of the lattice this model reduces to the FGM Hamiltonian:

$$H_{FGM}[\Delta(x)] \; = \; \sum_{\sigma} \int dx \, \Psi_{\sigma}^{\dagger}(x) \left(\frac{v_F}{i} \sigma_3 \frac{d}{dx} + \Delta(x)\sigma_1 \right) \Psi_{\sigma}(x) \; . \tag{2.89}$$

Here, we use again the spinor notation Eq. (2.22) to describe left- and right-moving electrons with spin σ and Fermi velocity v_F. The order parameter $\Delta(x) = \Delta_0 + \eta(x)$ contains the disorder fluctuation $\eta(x)$, which we assume to obey Gaussian white-noise statistics: $\langle \eta(x)\eta(y) \rangle = A\delta(x-y)$.

A crucial phenomenological assumption is made when the one-dimensional FGM is applied to describe Peierls materials: Interchain interactions between the Peierls chains are assumed to be so strong, that the Peierls order parameter does not deviate significantly from its average value Δ_0. It is, therefore, important to realize that the FGM does not treat the lattice degrees
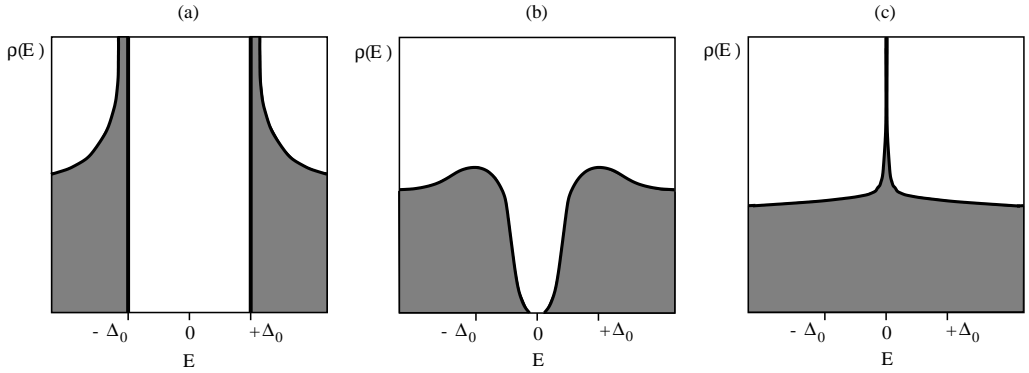
Figure 2-9: *Qualitative plot of the disorder-averaged density of electron states $\rho(E)$ in the FGM for three values of the disorder strength: (a) a perfect chain with $g = 0$, (b) a weakly disordered chain with $g < g_c$, and (c) a strongly disordered chain with $g > g_c$.*

of freedom in a self-consistent way when applied to a single Peierls chain. In other words, since the energy of the lattice is assumed to be constant and is neglected in H_{FGM}, the chain's lattice configuration is not allowed to adjust to the electronic disorder fluctuation $\eta(x)$. As we saw in Section 2.2 within the Takayama−Lin-Liu−Maki (TLM) model for perfect Peierls chains, for example, a soliton in the otherwise perfectly dimerized lattice represents a self-consistent solution of the order parameter $\Delta(x)$. These topological excitations are not described by H_{FGM}. However, as we briefly discuss below, solitons, albeit of a different nature, play an important role in the FGM as well.

We first discuss the disorder-averaged density of electron states in the FGM, $\rho(E)$, which has been studied numerically [23] and was even calculated analytically by Ovchinnikov and Erikhman [6]. In the analytical approach a mapping was used by which the equations describing the one-dimensional electron motion are reduced to a stochastic equation of Langevin type. The probability distribution to calculate the disorder average is then obtained from the stationary solution of the corresponding Fokker-Planck equation. For nonzero disorder the density of electron states close to the Fermi energy, $|E| \ll \Delta_0$, has the energy dependence

$$\rho(E) \propto \left| \frac{E}{\Delta_0} \right|^{\frac{2}{g} - 1} , \tag{2.90}$$

where the dimensionless parameter

$$g = \frac{A}{v_F \Delta_0} \tag{2.91}$$

is proportional to the disorder strength A [6]. We note that the symmetry property $\rho(E) = \rho(-E)$ follows from the charge conjugation symmetry of the FGM Hamiltonian Eq. (2.89). Furthermore, as can be seen from Eq. (2.90), the behavior of $\rho(E)$ is qualitatively different for g smaller or larger than $g_c = 2$. We plot $\rho(E)$ in Figure 2-9 for three different values of the disorder strength. A perfect Peierls chain $(g = 0)$ has an energy gap in the single-electron spectrum with $\rho(|E| < \Delta_0) = 0$. This energy gap becomes filled in the presence of disorder,

however, the density of disorder-induced electron states that occur inside the gap is small for weak disorder with $g < g_c$, leading to a pseudogap. For $g = g_c$, the density of states Eq. (2.90) is constant and the former energy gap is completely filled with electron states. If the disorder strength is large, $g > g_c$, the density of states is found to diverge at the Fermi energy $E = 0$. We note that this singularity is a consequence of the charge conjugation symmetry of the random Hamiltonian Eq. (2.89) and is not related to the probability properties of $\Delta(x)$ [24].

A large disorder fluctuation $\eta(x)$ is required in order to create an electron state with energy $E \ll \Delta_0$ close to the middle of the pseudogap. The "saddle-point" method has been used in Refs. [25, 26] to calculate the least suppressed disorder fluctuation $\bar{\eta}(x)$ among the required large fluctuations. Here, we estimate the form of $\bar{\eta}(x)$ restricting our considerations to the limit of weak disorder, $g \ll g_c$, where the density of disorder-induced states is strongly suppressed [25]. The weight of the disorder realization $\eta(x)$,

$$w[\eta(x)] = \exp\left(-\mathcal{S}[\eta(x)]\right) , \tag{2.92}$$

contains the suppression factor

$$\mathcal{S}[\eta(x)] = \frac{1}{2A} \int dx\, \eta(x)^2 - \gamma\left(\bar{E}[\eta(x)] - E\right) , \tag{2.93}$$

which has to be minimized with respect to $\eta(x)$. The first term in Eq. (2.93) stems from the the Gaussian weight, $p[\eta(x)] = \exp(-\frac{1}{2A}\int dx \eta(x)^2)$, while the second term with the Lagrange multiplier γ ensures that the energy of this particular disorder realization, $\bar{E}[\eta(x)]$, equals E. From the minimization of $\mathcal{S}[\eta(x)]$ we obtain for the optimal fluctuation $\bar{\eta}(x)$ the condition

$$\bar{\eta}(x) = \gamma A \sum_\sigma \bar{\Psi}_\sigma^\dagger(x)\, \sigma_1\, \bar{\Psi}_\sigma(x) , \tag{2.94}$$

where $\bar{\Psi}_\sigma(x)$ is the spinor of the state with energy $\bar{E}$. The solution of Eq. (2.94) with intragap electron states $\bar{\Psi}_{\sigma,\pm}(x)$ of the form Eq. (2.87) can be written as [25]:

$$\bar{\eta}(x) = -\Delta_0 k_0 \xi_0 \left[\tanh\left(k_0\left(x + \frac{R}{2}\right)\right) - \tanh\left(k_0\left(x - \frac{R}{2}\right)\right)\right] . \tag{2.95}$$

Here, $\xi_0 = v_F/\Delta_0$ is the characteristic length and k_0 is determined by $k_0 \xi_0 = \tanh(k_0 R)$ depending on the spatial extent R of the disorder fluctuation. Thus, the Peierls order parameter $\bar{\Delta}(x) = \Delta_0 + \bar{\eta}(x)$ of the least suppressed disorder fluctuation Eq. (2.95) has the form of a soliton-antisoliton pair as given by Eq. (2.85). The corresponding spectrum of electron states consists of a valence band with highest energy $-\Delta_0$, a conduction band with lowest energy $+\Delta_0$, and two localized intragap states $\bar{\Psi}_{\sigma,\pm}(x)$ with energies $\pm\bar{E}(R) = \pm\Delta_0/\cosh(k_0 R)$.

Next, we estimate the density of disorder-induced states taking only the least suppressed fluctuations $\bar{\eta}(x)$ into account. The spatial extent R of the soliton-antisoliton pair is fixed by the condition $\bar{E}(R) = E$ and depends for $E \ll \Delta_0$ logarithmically on the energy splitting: $R \approx \xi_0 \ln|2\Delta_0/E|$. It then follows from Eq. (2.93), that also the suppression factor depends logarithmically on the energy,

$$\mathcal{S}[\bar{\eta}(x)] \approx \frac{2v_F \Delta_0}{A} \ln\left|\frac{2\Delta_0}{E}\right| , \tag{2.96}$$

resulting in the weight

$$w[\bar{\eta}(x)] \; \propto \; \left| \frac{E}{\Delta_0} \right|^{\frac{2}{g}} \tag{2.97}$$

of the "saddle-point" configuration Eq. (2.95). Thus, in the weak disorder limit $g \ll 1$, the weight Eq. (2.97) provides a reasonable estimate for the energy dependence of the density of states inside the pseudogap. Moreover, performing a Gaussian integration over disorder fluctuations $\eta(x)$ close to the soliton-antisoliton "saddle-point" configuration $\bar{\eta}(x)$ results in the expression [26]:

$$\rho(E) \; = \; \frac{e}{\pi v_F \, g} \left| \frac{eE}{2\Delta_0} \right|^{\frac{2}{g} - 1} \; . \tag{2.98}$$

It may be concluded from the thus obtained correct exponent for the energy dependence of $\rho(E)$, that for all values of g the typical form of the disorder fluctuation with $|E| \ll \Delta_0$ is close to that of a soliton-antisoliton pair as given by Eq. (2.95).

While in the FGM it is the typical form of the disorder-induced electron states which resembles the superposition of soliton and antisoliton midgap states, the above considerations motivate the question whether disorder can also induce solitons in the lattice dimerization of a Peierls chain. We mentioned already before, that the lattice degrees of freedom of a single Peierls chain are not treated self-consistently within the FGM. In contrast, the lattice configuration of a Peierls chain which is described by the Hamiltonian Eq. (2.30) is allowed to adjust to the electronic disorder fluctuation $\eta(x)$. In Chapter 3 we study the effect of the electronic disorder on the lattice degrees of freedom in a single Peierls chain within this model. We find, in fact, that neutral solitons are induced by the disorder in the chain's lattice dimerization with a density that is proportional to the disorder strength A. Weak interchain interactions in quasi-one-dimensional Peierls systems are taken into account in Chapter 5 and give rise to an exponential suppression of this soliton density. For strong enough interchain interactions the Peierls order parameter is given by its average value Δ_0 approaching the phenomenological limit where the FGM is valid.

2.4 Residual interactions

It is a characteristic feature of Peierls systems, that the coupling between the conduction electrons and the lattice dominates other interactions, and it is in this sense, that we consider electron correlations and interchain interactions as residual interactions in Peierls systems. We discuss in Section 2.4.1 the effects of electron correlations in a single Peierls chain, while interactions between the Peierls chains are considered in Section 2.4.2.

2.4.1 Effects of electron correlations

It was first found for non-interacting electrons in the absence of disorder that the (half-filled) Peierls chain reaches its minimal energy in either one of two uniformly dimerized configurations $\Delta_{lat}(x) = \pm \Delta_0$ [3]. A model which, in addition to electron-lattice interactions, includes

electron-electron interactions due to both short- and long-range Coulomb forces is hard to solve. This is in particular true for (quasi-) one-dimensional systems where strong fluctuations often cause mean-field methods to fail and the complexity of the full many-body problem must be faced.

In this section we consider the extended Peierls-Hubbard model, where electron correlations are taken into account explicitly by the on-site Coulomb repulsion, U, and nearest neighbor Coulomb repulsion, V. Here, U and V are to be understood as effective parameters, since the interaction between electrons at more distant sites (or in neighboring chains) is neglected. In what follows, we will summarize several known results for the charge gap E_g and the lattice dimerization Δ_{lat} in the parameter space $\{U/W, V/W, \lambda\}$ of the extended Peierls-Hubbard model. Here, W denotes again the free electron band width and is a measure for the kinetic energy of the non-interacting electrons, while λ is the dimensionless electron-lattice coupling constant introduced in Eq. (2.29).

In the absence of the electron-lattice interaction ($\lambda = 0$) a separation between charge and spin degrees of freedom takes place in the half-filled Hubbard chain ($V = 0$). While the spin excitations remain gapless, there is a finite charge gap E_g for (positive) U with the asymptotic behavior

$$
E_g \approx
\begin{cases}
4\pi^{-1}(UW)^{1/2}e^{-\pi W/(2U)} & \text{for} \quad U \ll W \\[2ex]
U\left(1 - \frac{W}{U}\right) & \text{for} \quad U \gg W
\end{cases}
\tag{2.99}
$$

and the half-filled one-dimensional system is called a Mott-Hubbard insulator [27, 28, 29].

If we switch on the electron-lattice interaction ($\lambda \neq 0$), the Peierls instability will nevertheless occur in the (extended) Peierls-Hubbard model, since the lattice dimerization can still lower the total chain energy due to the opening of a gap in the spectrum of spin excitations. Depending on the strength of the interactions, however, several limits have to be distinguished.

In the limit $U \gg W$, the size of the charge gap is much larger than the size of the gap in the spin excitations and the system turns into a spin-Peierls system in which the dimerized state results from the interaction between the lattice and the spins of the electrons. The lattice dimerization is then approximately given by

$$
\Delta_{lat} \approx \frac{W}{2}\left(\frac{\lambda W}{8U}\right)^{3/2} \qquad \text{for} \quad V \ll W \ll U
\tag{2.100}
$$

and is a decreasing function of U [30]. For weak to intermediate on-site Coulomb repulsion, $0 < U < W$, there are still two regimes to be distinguished according to the relative importance of electron-electron and electron-lattice interactions. If the electron-electron interactions dominate over the electron-lattice interactions, $U/W \gg \lambda$, the system has to be considered as a Mott-Hubbard insulator in which the additional coupling to the lattice stabilizes the bond order wave (BOW). In this case the lattice dimerization appears only as a secondary effect and is approximately given by

$$
\Delta_{lat} \approx 2U\left(\frac{\lambda W}{8U}\right)^{3/2} e^{-\pi W/(2U)} \qquad \text{for} \quad V \ll U < W \,,
\tag{2.101}
$$

while the charge gap is essentially a correlation gap [28, 31]. If, however, the electron-lattice interaction dominates, $\lambda \gg U/W$, the ground state can be characterized as a Peierls semi-conductor, where the electron-electron interactions provide only small renormalizations of the pre-existing Peierls gap and the lattice dimerization. The lattice dimerization is then approximately given by the mean-field result [7]

$$\Delta_{lat} \approx \frac{\lambda W}{\lambda + 4V/(\pi W)} \, e^{-1/(\lambda + (4V/\pi W))} \qquad \text{for } V \ll U \ll W \, . \tag{2.102}$$

Thus, small nearest-neighbor Coulomb repulsion, $V \ll U$, results in an enhancement of the lattice dimerization. If $V \sim U/2$, however, a BOW-CDW instability border is reached and the lattice dimerization is lost on increasing V. Instead, the system is characterized by an imaginary order parameter and favors a charge density wave where the occupation of equidistant sites alternates between zero and two electrons [32]. In the absence of electron correlations ($U = V = 0$), the lattice dimerization Δ_{lat} reduces to the gap equation (2.55) of the TLM model (see Section 2.2.1) with

$$E_g \approx 2\Delta_{lat} \approx 2W \, e^{-1/\lambda} \tag{2.103}$$

the energy gap in the electronic spectrum [4]. To conclude this analytical walk through the parameter space of the extended Peierls-Hubbard model we note, that the lattice dimerization survives at all values of U and $V \ll U$. Numerical calculations beyond the mean-field level reveal, that the BOW does not only survive at all values of U and $V < U/2$, but show that the lattice dimerization is enhanced when U and V increase and reaches a maximum around $U \sim W$ and $V \sim U/2$ [32].

We finally discuss electron correlation effects in the conjugated polymer *trans*-polyacetylene. In this material the charge gap, as probed in optical experiments, can not be attributed to either the electron-electron interaction or the electron-lattice interaction alone. Fitting the observed optical gap energy $E_g \approx 1.8$ eV [12] by Eq. (2.103) using solely electron-lattice interactions ($W \sim 10$ eV), requires a coupling constant $\lambda \sim 0.4$. However, a direct estimate of λ according to its definition Eq. (2.29) reveals a substantially smaller value $\lambda \sim 0.16$ [32]. On the other hand, a value of $U \sim W$ is required to fit the optical gap in the pure Hubbard model ($\lambda = 0$). Although this value is not unreasonable, the observed existence of dimerization with $u/a \sim 3\%$ [9, 10] requires electron-lattice interactions. A detailed analysis of experimental and theoretical results for *trans*-polyacetylene reveals that the reasonable ranges of the on-site and nearest neighbor Coulomb repulsion are given by, respectively, $W/4 < U < W$ and $W/8 < V < W/3$ [32].

The relative importance of the electron-electron and the electron-lattice interaction is still a controversial issue in this field and it seems likely that both interactions give about equal contributions to the optical gap in this conjugated polymer. On the other hand, it is important to note that the lattice dimerization survives electron correlations in *trans*-polyacetylene. It thus follows, that also topological excitations such as neutral solitons will persist, while the precise form of the electron-electron interactions is only important to the extent that it determines the value of Δ_0 and the creation energy of the topological excitations [33, 34].

2.4.2   Effects of interchain coupling

Real Peierls systems are - in contrast to the extensively studied one-dimensional models - inherently three-dimensional and the interaction between the chains plays an important role. Fluctuations create domain walls (solitons) that connect the two degenerate bond alternation patterns which are characterized by the chain dimerization $\Delta_{lat} = \pm \Delta_0$. A soliton density, however small, will destroy the long-range bond order in a one-dimensional chain. In a three-dimensional arrangement of chains, however, even an interchain coupling that is weak compared with the intrachain coupling will serve to stabilize a long-range bond order wave against (thermal or disorder) fluctuations. Several possible mechanisms producing interchain coupling exist, such as Coulomb interaction between bond charges or interchain electron tunnelling, and they determine the type of three-dimensional ordering with respect to the chain dimerizations. The chains are ordered in phase if the lattice dimerization $\Delta_{lat,i}$ of the i'th chain equals the lattice dimerizations of its $j = 1, 2, \ldots, Z$ neighboring chains, $\Delta_{lat,i} = \Delta_{lat,j}$. On the other hand, the chains are ordered in anti-phase if $\Delta_{lat,i} = -\Delta_{lat,j}$.

We first discuss the interchain coupling due to electron tunnelling between two chains. Using the spinor notation Eq. (2.22) to describe the right- and left-moving electron fields in chain $i = 1, 2$ by $\Psi_{i,\sigma}(x)$, the interaction Hamiltonian is given by

$$H_\perp \; = \; -t_\perp \int dx \left[\Psi_{1,\sigma}^\dagger(x) \, \Psi_{2,\sigma}(x) \, + \, \Psi_{2,\sigma}^\dagger(x) \, \Psi_{1,\sigma}(x) \right] \; , \tag{2.104}$$

with the electron hopping amplitude $t_\perp$ between the chains. The quasi-one-dimensional nature of Peierls systems with $t_\perp \ll t_0$ suggests that $H_{res} = H_\perp$ can be treated as a perturbation in the Hamiltonian Eq. (2.30). To lowest order in the interchain electron hopping the correction to the ground state energy per unit length becomes

$$\Delta E_\perp / L \; \approx \; -\frac{t_\perp^2}{\pi \, t_0 \, a} \frac{1}{2} \left(1 - \frac{\Delta_{lat,1}}{\Delta_0} \frac{\Delta_{lat,2}}{\Delta_0} \right) \; , \tag{2.105}$$

where the chains are assumed to be perfectly dimerized in the absence of disorder, $|\Delta_{lat,1}| = |\Delta_{lat,2}| = \Delta_0$ [35]. The energy correction $\Delta E_\perp$ depends on the relative sign of the chain dimerizations and the preferred chain ordering is anti-phase. It can be readily understood that this ordering is preferred by looking at the tight-binding model for a two-dimensional array of chains. The corresponding electron energy spectrum is given by

$$\varepsilon_{2D}(k, k_\perp) \; = \; -2\, t_0 \cos(ka) - 2\, t_\perp \cos(k_\perp b) \; , \tag{2.106}$$

where the momentum $k_\perp$ belongs to the transverse direction and b denotes the interchain spacing. The Peierls instability occurs for phonons with momentum $\vec{Q} = (q, q_\perp)$ that fulfill the nesting condition $\varepsilon_{2D}(k + q, k_\perp + q_\perp) = \varepsilon_{2D}(k, k_\perp)$. The backward-scattering of electrons in the chains with momentum $q = 2k_F = \pi/a$ requires, thus, a transverse phonon momentum $q_\perp = \pi/b$ which, in fact, corresponds to an anti-phase ordering of the bond alternation in neighboring chains.

The creation of solitons in a chain that is embedded in a three-dimensional system of chains, leads to a mismatch of the chains' bond alternations. It follows from Eq. (2.105) that the interchain interactions restore the long-range bond order, since per unit length a confinement

energy

$$E_c \;=\; \frac{Z\,t_\perp^2}{\pi\,t_0\,a} \tag{2.107}$$

is associated with a mismatched domain in a chain which is surrounded by Z neighboring chains. Thus, the interchain interactions confine solitons into pairs by a potential $V_c = E_c l$ that grows linearly with their pair size l. This soliton confinement is due to the fact that the energetic degeneracy of the two bond alternation patterns in an isolated chain ($\Delta_{lat} = \pm\Delta_0$) is removed by the interchain interactions.

In the case of the conjugated polymer *trans*-polyacetylene, the experimental situation concerning the bond alternation ordering in the (partially) crystalline samples is at present not definitive [36, 37]. While it is accepted that *trans*-polyacetylene has a (pseudo-) hexagonal unit cell, there is still considerable disagreement whether neighboring carbon chains are dimerized in phase ($P2_1/a$ space group) or in anti-phase ($P2_1/n$ space group). Taking into account that neighboring chain planes are tilted with respect to each other by a large angle of about $70°$ has important consequences for the interchain hopping amplitude $t_\perp$. In general, the hopping amplitudes depend strongly on the relative directions of the two orbitals involved and on the spatial vector connecting the two sites. Geometrical considerations for *trans*-polyacetylene reveal that the interchain hopping amplitude alternates along the chains in size and possibly even in sign [38, 39]. If the relative signs of subsequent interchain hopping amplitudes are different, the space group is $P2_1/a$ instead of $P2_1/n$. It is difficult to estimate the interchain hopping amplitudes reliably. From band structure calculations which account only for a single interchain hopping amplitude, one obtains $t_\perp \sim 0.03 t_0$ [40]. Using $t_0 \sim 2.5$ eV one obtains a confinement energy $E_c \sim 15$ K$/a$ for a pair of chains ($Z = 2$). This value should be compared with the confinement energy due to other mechanisms that produce interchain coupling. For example, the confinement energy due to the Coulomb interaction between the bond charges of two chains has been estimtated to be only of the order $E_c \sim 0.15$ K$/a$. However, this type of coupling leads to an in phase ordering of the chains and, thus, to some extent counteracts the anti-phase ordering due to interchain electron tunnelling [41]. We also note that the electron-lattice interaction between chains has been taken into account in numerical pseudopotential calculations and the resulting space group for crystalline *trans*-polyacetylene is expected to be $P2_1/a$ [42].

In Chapter 5 we will account for weak interchain interactions in disordered Peierls systems to study the magnetic response due to disorder-induced neutral solitons. For sufficiently strong interchain interactions the system is in a bond-ordered phase. At the same time, the anisotropy $t_\perp \ll t_0$ allows one to treat the interchain interactions in a mean-field way where H_{res} in the Hamiltonian Eq. (2.30) is given by

$$H_{int} \;=\; \bar{W}\,\frac{\langle\langle\Delta_{lat}(x)\rangle\rangle}{\Delta_0} \int dx\,\frac{\Delta_{lat}(x)}{\Delta_0}\;. \tag{2.108}$$

Here, $\bar{W} = E_c/2$ is the interaction energy per unit length and the double brackets of the average order parameter $\langle\langle\Delta_{lat}(x)\rangle\rangle$ denote both the thermal and the disorder average. Within the chain mean-field approach the relative ordering of neighboring chains with respect to their dimerizations depends on the sign of the confinement energy E_c.

Bibliography

[1] A.J. Heeger, S. Kivelson, J.R. Schrieffer, and W.P. Su, Rev. Mod. Phys. **60**, 781 (1988).

[2] W.P. Su, Solid State Commun. **42**, 497 (1982); E. Fradkin and J.E. Hirsch, Phys. Rev. B **27**, 1680 (1983); A. Auerbach and S. Kivelson, Phys. Rev. B **33**, 8171 (1986); M.V. Mostovoy and J. Knoester, Phys. Rev. B **53**, 12057 (1996); M.V. Mostovoy and J. Knoester, Phys. Rev. B **54**, 9784 (1996).

[3] R.E. Peierls, *Quantum Theory of Solids* (Oxford Univ. Press, London, 1955), p. 108.

[4] H. Takayama, Y.R. Lin-Liu, and K. Maki, Phys. Rev. **21**, 2388 (1980).

[5] P.A. Lee, T.M. Rice, and P.W. Anderson, Phys. Rev. Lett. **31**, 462 (1973).

[6] A.A. Ovchinnikov and N.S. Erikhman, Sov. Phys. JETP **46**, 340 (1977).

[7] D. Baeriswyl, in *Theoretical Aspects of Band Structures and Electronic Properties of Pseudo-One-Dimensional Solids, ed. by H. Kamimura* (D. Reidel Publishing Company, 1985), p. 1.

[8] T. Kennedy and E.H. Lieb, Phys. Rev. Lett. **59**, 1309 (1987).

[9] C.R. Fincher *et al.*, Phys. Rev. Lett. **48**, 100 (1982).

[10] C.S. Yannoni and T.C. Clarke, Phys. Rev. Lett. **51**, 1191 (1983).

[11] G. Grüner, *Density waves in solids* (Addison-Wesley, Reading, 1994).

[12] D. Moses *et al.*, Phys. Rev. B **26**, 2361 (1982).

[13] W.P. Su, J.R. Schrieffer, and A.J. Heeger, Phys. Rev. Lett. **42**, 1698 (1979); Phys. Rev. B **22**, 2099 (1980); Phys. Rev. B **28** 1138 (1983) (erratum).

[14] M.J. Rice, Phys. Lett. **71 A**, 152 (1979).

[15] P.J.S. Foot, N.C. Billingham, and P.D. Calvert, Synthetic Metals **16**, 265 (1986).

[16] W.P. Su, Solid State Commun. **35**, 899 (1980).

[17] D.K. Campbell and A.R. Bishop, Phys. Rev. B **24**, 4859 (1981); Nucl. Pys. B **200**, 297 (1982).

[18] K.Kim and D.H. Lee, to appear in Phys. Rev. B, cond-mat/9912146, (1999).

[19] B.C. Xu and S.E. Trullinger, Phys. Rev. Lett. **57**, 3113 (1986).

[20] K. Kim, R.H. McKenzie, and J.H. Wilkins, Phys. Rev. Lett. **71**, 4015 (1993).

[21] R. Hayn and J. Mertsching, Phys. Rev. B **54**, R5199 (1996).

[22] B. Starke and J. Mertsching, Synth. Met. **76**, 217 (1996).

[23] L. Bartosch and P. Kopietz, Phys. Rev. Lett. **82**, 988 (1999); L. Bartosch and P. Kopietz, cond-mat/9908065 (1999).

[24] F.J. Dyson, Phys. Rev. **92**, 1331 (1953).

[25] M.V. Mostovoy and J. Knoester, Phys. Lett. A **235**, 535 (1997).

[26] M.V. Mostovoy and J. Knoester, Int. J. Mod. Phys. B **13**, 1601 (1999).

[27] B. Horovitz and J. Sólyom, Phys. Rev. B **32**, 2681 (1985).

[28] V.Ya. Krivnov and A.A. Ovchinnikov, Sov. Phys. JETP **63**, 414 (1986).

[29] J. Voit and H.J. Schulz, Phys. Rev. B, **37**, 10068 (1988).

[30] M.C. Cross and D.S. Fisher, Phys. Rev. B **19**, 402 (1979); T. Nakano and H. Fukuyama, J. Phys. Soc. Jpn. **49**, 1679 (1980); J. Kondo, Physica **9B**, 176 (1980).

[31] A.A. Ovchinnikov and I.I. Ukrainskii, Sov. Sci. Rev. B, Chem. **9**, 125 (1987).

[32] *see for a review:* D. Baeriswyl, D.K. Campbell, and S. Mazumdar in *Conjugated Conducting Polymers, ed. by H.G. Kiess* (Springer-Verlag, 1992), p. 7.

[33] S. Kivelson and D.E. Heim, Phys. Rev. B **26**, 4278 (1982).

[34] D.K. Campbell, T.A. DeGrand, S. Mazumdar, Phys. Rev. Lett. **52**, 1717 (1984).

[35] D. Baeriswyl and K. Maki, Phys. Rev. B **28**, 2068 (1983).

[36] J.H.F. Martens *et al.*, Polymer **35**, 402 (1994).

[37] P.F. van Hutten and G. Hadziioannou, in *Organic Conductive Molecules and Polymers, ed. by H. S. Nalwa* (John Wiley & Sons, Chicester, UK, 1996).

[38] D. Baeriswyl and K. Maki, Phys. Rev. B **38**, 8135 (1988).

[39] K. Fesser, Phys. Rev. B **40**, 1962 (1989).

[40] P.M. Grant and I. P. Batra, J. Phys. **44** (C3), 431 (1983).

[41] S. Jeyadev, Phys. Rev. B **28**, 3447 (1983).

[42] P. Vogl and D.K. Campbell, Phys. Rev. Lett. **62**, 2012 (1989); P. Vogl and D.K. Campbell, Phys. Rev. B **41**, 12797 (1990).